Mon. Not. R. Astron. Soc. **000**, 1–16 (0000) Printed 21 December 2005 (MN LATEX style file v2.2)

High field strength modified ABC and rotor dynamos.

Robert Cameron[1⋆] and David Galloway[2]†

[1] *Max-Planck-Institut für Sonnensystemforschung, Max-Planck-Straße 2, D-37191 Katlenburg-Lindau, Germany*

[2] *School of Mathematics and Statistics, University of Sydney, NSW 2006, Australia*

ABSTRACT

The Archontis dynamo was the first stationary dynamo discovered which saturates with almost equal magnetic and kinetic energies in the limit of large Reynolds numbers (Archontis 2000; Dorch & Archontis 2004; Archontis et al. 2005; Cameron & Galloway 2005). In this paper we present two further examples, one based on a series of numerical calculations, the other on the analytic rotor dynamos of Herzenberg (1958). The forcing and flow in these new examples lack some of the symmetries of the Archontis dynamo are therefore more generic. The saturation mechanism is thus not a unique property of the Archontis dynamo.

For the numerical solutions, we also have investigated the structure and stability of the flow and field near the stagnation points and those streamlines which enter and leave them. These structures play an important part in the operation of the dynamo mechanism, and the way they interact with one another is mirrored in the analytic example based on the Herzenberg rotors.

Key words: MHD; magnetic fields.

1 INTRODUCTION

Magnetic fields are believed to exist in many astrophysical systems, including some planets, most stars, and all galaxies. In most cases these are believed to be the result of dynamo action, and it is now reasonably clear that any sufficiently complicated flow is likely to produce a magnetic field. The next important question that arises is whether the fields thus generated are strong enough to be comparable with what is observed.

⋆ E-mail: cameron@linmpi.mpg.de
† E-mail: dave@maths.usyd.edu.au

In the case of the Earth, the total magnetic energy substantially exceeds the kinetic energy of motions within the Earth's core. For the Sun, the magnetic energy has been estimated by Steiner & Ferriz-Mas (2005) to be 5×10^{32} Joules, which they assert is comparable with the 1×10^{33} Joules of available kinetic energy associated with the differential rotation in the convection zone. Lastly, Beck (2002) reviews the energy budget for galaxies, and finds that the energy density of the magnetic field is comparable to the energy density of the turbulent motions. He also reports that the energy density associated with galactic rotation is about 400 times greater. To take a concrete example, the magnetic energy density of the interstellar material near the Sun is given as approximately 2×10^{-13} Joules/m^3 and the kinetic energy density of the turbulence as 4×10^{-13} J/m^3. The energy associated with the rotation of this material with the Galaxy is around 400 times larger, but it is not clear if all the energy due to the galactic rotation is available to power the dynamo.

The observations thus suggest that in planets, stars and possibly galaxies, the total magnetic energy is often comparable to the available kinetic energy. One is then led to ask what theory might say about possible field strength levels. In recent years this has been a very active area of debate. Dynamo theory before about 1990 was mainly considered from a kinematic point of view. In this, the velocity field is prescribed and the induction equation is solved to determine the linear growth or decay rate of the magnetic field, growth being indicative of dynamo action. Such an approach can never determine the final field strengths, which are governed by the opposition provided by the essentially nonlinear Lorentz force in the momentum equation (Lenz's Law). In astrophysics the Reynolds number Re and the magnetic Reynolds number Rm (a non-dimensional measure of electrical conductivity) are huge; typical values of the latter might be 10^3 for the Earth, 10^8 for the Sun, and 10^{19} for galaxies. Various authors (Vainshtein & Cattaneo 1992; Gruzinov & Diamond 1994; Diamond et al. 2005) have argued that in the high Reynolds number limit the filamentary nature of the magnetic field means that its strength will be restricted to levels far below what is observed (see also Galloway, 2003). Others have vociferously opposed this contention (see Brandenburg 1994; Blackman 2002; Blackman & Field 2002). This debate has proceeded mostly within the context of mean field electrodynamics; the latter is the only real tool available for direct application of dynamo theory to specific astrophysical objects (see eg Rüdiger and Hollerbach 2004), and even then it requires some ad hoc recipe to limit the field strength. The validity of the various proposed recipes is what is at the heart of the debate. In the mean field approximation, one parametrises the turbulence through two quantities α

and β, and the question is whether α and β are "quenched" in the high magnetic Reynolds number limit.

In the last fifteen years, computers have evolved to the extent that direct numerical solution of the governing equations has become a viable tool, at least at moderate Reynolds numbers. For the Earth, the latter are low enough that it is now possible to tackle the above question computationally, and simulations have shown that a total magnetic energy which exceeds the total kinetic energy is possible (Glatzmaier & Roberts 1995). For the Sun, stars, and galaxies the Reynolds numbers are beyond the range of what can be directly calculated, and we must therefore use some modelling of the small scales. In all cases substantial problems exist. Simulations performed with Rm in the low thousands must be extrapolated up to $\mathrm{Rm} = 10^{19}$. Additionally the code must be ran for many diffusive timescales (Hughes 1993) to have confidence that the solutions are not transients. With these caveats, the results from studies with both non-helical (Maron et al. 2004; Haugen et al. 2004) and helical (Brandenburg 2001) forcings indicate that saturation can occur with magnetic energies comparable to or in excess of the kinetic energy, apparently independently of Rm and Re.

In this paper we step sideways and consider dynamos that are *not* filamentary, and which have the property that the velocity and magnetic field become perfectly aligned and have similar energies when Re and Rm are large. We will refer to such objects as $\mathbf{U} \sim \mathbf{B}$ dynamos. The first to be discovered was the Archontis dynamo (Archontis 2000; Dorch & Archontis 2004; Archontis et al. 2005, also studied at length in Cameron & Galloway 2005). The current work extends the study in that paper to consider a wider class of driving forces, with the aim of addressing the following issues: Is the stability of the Archontis dynamo unique? Do time dependent $\mathbf{U} \sim \mathbf{B}$ solutions exist? Is the existence of heteroclinic orbits (separator lines connecting different stagnation points, which are present in the Archontis dynamo and seem to play a key role) an essential ingredient of $\mathbf{U} \sim \mathbf{B}$ dynamos? Finally, if there are topologically important orbits, what determines the properties of the dynamo in their neighbourhoods?

To answer the first three of these questions, in section 3 we look at a numerical example with fewer symmetries than the Archontis case. The last question is addressed by considering a purely analytic example in section 4. This is based on the scaling arguments given in Cameron & Galloway (2005), applied to the rotor dynamos of Herzenberg (1958) and Gibson (1968a), and provides an example of an analytically derived family of strong-field dynamos, albeit one with a very specific type of forcing. These solutions exist for arbitrarily high Rm

and Re, although so far we have been unable to determine whether or not they are stable. In Cameron & Galloway (2005) we studied the Archontis dynamo, and showed numerically that it was stable for a range of diffusivities; We also argued heuristically that it is likely to be stable for all higher Reynolds numbers, at least in the case where the two diffusivities are equal. That one example enables us to say that dynamos which saturate with equal magnetic and kinetic energies are possible. It does not indicate whether such dynamos are common. In this paper we give further examples to suggest that such behaviour may turn out to be quite widespread, and that it may be worth observers attempting to determine whether $\mathbf{U} \sim \mathbf{B}$ in real astrophysical objects.

2 EQUATIONS

Astrophysical plasmas exist in a variety of different environments and many microphysical processes can be important in different cases. In this paper we take the simplest version of Ohm's law in a moving medium, with just an ordinary resistivity, and we restrict ourselves to an incompressible fluid. This approach is the usual one in dynamo theory, but it should be noted that there are astrophysical situations where other terms such as the Hall effect are likely to be important. The equations (in SI units) are then the Navier-Stokes equation including the Lorentz force,

$$\begin{aligned}\frac{\partial \mathbf{u}}{\partial t} &+ \nabla \cdot (\mathbf{u}\mathbf{u}) = -\nabla P/\rho \\ &+ \frac{1}{\mu_0 \rho}(\nabla \times \mathbf{B}) \times \mathbf{B} + \nu \nabla^2 \mathbf{u} + \mathbf{F}\,; \end{aligned} \tag{1}$$

the induction equation,

$$\frac{\partial \mathbf{B}}{\partial t} = \nabla \times (\mathbf{u} \times \mathbf{B}) + \eta \nabla^2 \mathbf{B}\,, \tag{2}$$

the continuity equation for an incompressible fluid,

$$\nabla \cdot \mathbf{U} = 0\,, \tag{3}$$

and the solenoidality condition,

$$\nabla \cdot \mathbf{B} = 0\,. \tag{4}$$

Here η and ν are the viscous and magnetic diffusivities, $\mathbf{F}$ is the applied driving force, and ρ is the density. The gas pressure P is determined by the requirement that $\nabla \cdot \mathbf{U} = 0$, so that no energy equation or equation of state is necessary.

In section 3 we perform a simulation using a periodic cube: in dimensional units we

define the length of each side of the box to be $2\pi L$. Associated with physical systems there will also be a characteristic (dimensional) speed U_0. This allow us to nondimensionalise the remaining equations. We scale density by $1/\rho_0$, length by $1/L$, time by L/U_0, where U_0 is a velocity which for the moment we leave unspecified, and magnetic field by $\sqrt{\rho_0\mu_0}/U_0$. The equations then take the form

$$\frac{\partial\bar{\mathbf{B}}}{\partial\bar{t}} = (\bar{\mathbf{B}}\cdot\bar{\nabla})\bar{\mathbf{U}} - (\bar{\mathbf{U}}\cdot\bar{\nabla})\bar{\mathbf{B}} + \bar{\eta}\bar{\nabla}^2\bar{\mathbf{B}} \tag{5}$$

$$\frac{\partial\bar{\mathbf{U}}}{\partial\bar{t}} = -(\bar{\mathbf{U}}\cdot\bar{\nabla})\bar{\mathbf{U}} + (\bar{\mathbf{B}}\cdot\bar{\nabla})\bar{\mathbf{B}} + \bar{\nu}\bar{\nabla}^2\bar{\mathbf{U}} + \bar{\mathbf{F}} - \bar{\nabla}\bar{P} \tag{6}$$

$$\bar{\nabla}\cdot\bar{\mathbf{U}} = \bar{0} \tag{7}$$

$$\bar{\nabla}\cdot\bar{\mathbf{B}} = \bar{0} \tag{8}$$

where the bars indicate non-dimensional quantities, and $\bar{P}$ now includes the magnetic pressure. We use the non-dimensional form of the equations exclusively hereafter, and for notational convenience suppress the bars on the understanding that variables refer to their non-dimensional versions.

The numerical methods we have used are standard and are briefly described in Cameron & Galloway (2005). The tests we have used to check the code are also described there.

3 RESULTS

Our numerical results concern a dynamo which is driven by the external forcing

$$\mathbf{F}_\gamma = \nu \begin{pmatrix} A\sin z + C\gamma\cos y \\ B\sin x + A\gamma\cos z \\ C\sin y + B\gamma\cos x \end{pmatrix}. \tag{9}$$

When $\gamma = 1$ this is the well-studied ABC forcing (Galanti et al. 1992), and when $\gamma = 0$ and $A = B = C$ it is the forcing for the Archontis dynamo. The former case is not further considered here because the ABC flow is Beltrami, with $\mathbf{U}\times(\nabla\times\mathbf{U}) = \mathbf{0}$. Since $\mathbf{U}\sim\mathbf{B}$ dynamos involve a balance between $\mathbf{U}\times(\nabla\times\mathbf{U})$ and $\mathbf{B}\times(\nabla\times\mathbf{B})$ in the momentum equation, Beltrami flows are unlikely to give rise to them, and certainly no such examples have yet been found. To have a system with less symmetry and non-Beltrami forcing, we have taken $\gamma = 0.125$ and $A : B : C = 0.5 : 1 : 1$. Results using this forcing are described in section 3.1, and in particular when $\eta = \nu = 1/100$ we find a stable, time-independent solution.

In Cameron & Galloway (2005) we showed how new $\mathbf{U}\sim\mathbf{B}$ dynamos can be constructed

from any time-independent solution to the induction equation. Therefore in section 3.2 we begin with the stable stationary solution found in section 3.1 at $\eta = \nu = 1/100$ and generate a new steady dynamo for $\eta = \nu = 1/400$. Our numerical calculations show that this new state is unstable, but remarkably the system evolves to a third nearby equilibrium which significantly differs from the unstable state only near the stagnation points and their 1-D unstable manifolds. This third equilibrium appears to be stable. The processes governing the behaviour in these regions can be understood using an analytic model based on the 'rotor dynamo' solutions to the induction equation, due to Herzenberg (1958) and Gibson (1968b). The corresponding analysis is given in section 4.

3.1 Modified ABC forcing

Our first computation was performed with $\eta = \nu = 1/100$. We used the initial condition $\mathbf{U} = \mathbf{B} = \mathbf{F}_\gamma/\nu$ [1]. A small amount of noise satisfying $\nabla \cdot \mathbf{B} = \nabla \cdot \mathbf{U} = 0$ was added in order to speed up the evolution of any instability. Figure 1 shows the evolution of the kinetic and magnetic energies. After a brief transient they evolve to similar steady state values.

It is useful to consider the problem in terms of the Elsasser variables $\mathbf{\Lambda}_+ = \mathbf{U} + \mathbf{B}$ and $\mathbf{\Lambda}_- = \mathbf{U} - \mathbf{B}$. These equilibrate at very different levels, with $\mid \mathbf{\Lambda}_+ \mid^2$ having a maximum value (over the box) of 0.96, compared to a maximum of 0.045 for $\mid \mathbf{\Lambda}_- \mid^2$. This is similar to what occurs for the Archontis dynamo (Cameron & Galloway 2005), but the spatial structures of $\mathbf{\Lambda}_+$ and $\mathbf{\Lambda}_-$, shown in Figures 2 and 3 demonstrate that the solutions have far less symmetry. It can also be seen that both $\mathbf{\Lambda}_+$ and $\mathbf{\Lambda}_-$ occupy a relatively large fraction of the volume. In fact, there *are* significant filamentary regions, but because they are places where the scaling with $\nu = \eta$ is different to what it is in the rest of the domain, rather than regions where Λ_+ or Λ_- are particularly large, they do not show up in these plots. We will return to this point in Section 3.2.

Since the system evolves to a time independent equilibrium, it is possible to construct new equilibria with higher Reynolds and magnetic Reynolds numbers (Cameron & Galloway 2005). If $\mathbf{U_0}$ and $\mathbf{B_0}$ are the equilibrium values when $\eta = \nu = \nu_0$, then for new diffusivities $\eta = \nu = \epsilon\nu_0$, the force

$$\mathbf{F} = \epsilon^2(\mathbf{U_0} \cdot \nabla \mathbf{U_0} - \nu_0 \nabla^2 \mathbf{U_0}) + 2\epsilon \mathbf{B_0} \cdot \nabla \mathbf{U_0} \tag{10}$$

[1] Because $\mathbf{U}$ and $\mathbf{F}$ are vectors, whereas $\mathbf{B}$ is a pseudo-vector, we hereafter specify the use of a right-handed coordinate system. Since the dynamo problem is invariant under the transformation $\mathbf{B} \rightarrow -\mathbf{B}$ this point is not critical.

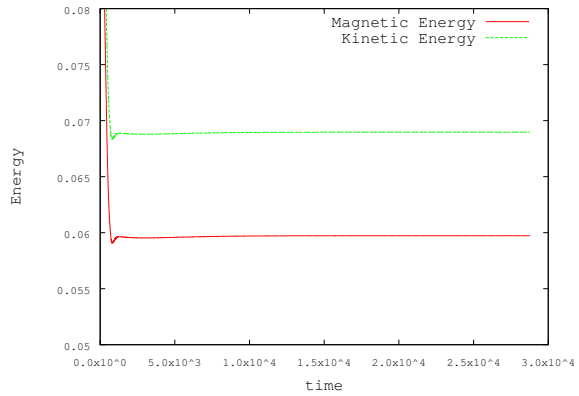

Figure 1. The magnetic and kinetic energies for the case $\gamma = 0.125$, $A : B : C = 0.5 : 1 : 1$, $\nu = \eta = 1/100$, plotted as a function of time.

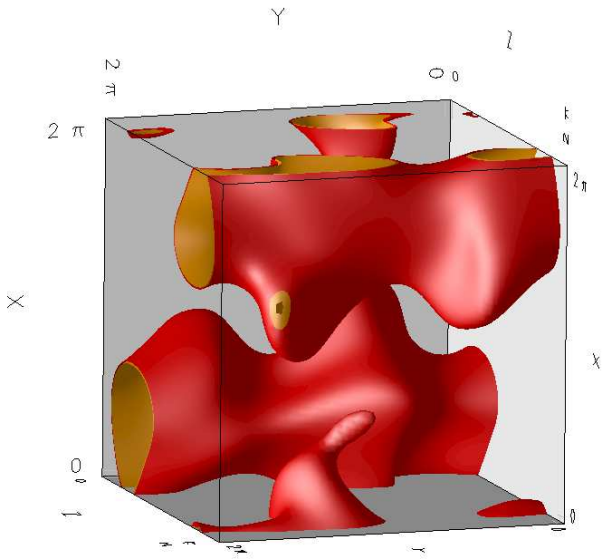

Figure 2. The equilibrium structure of $\mathbf{\Lambda}_+$ for the forcing $\mathbf{F}_\gamma = \nu\{A\sin z + C\gamma\cos y, B\sin x + A\gamma\cos z, C\sin y + B\gamma\cos x\}$, with the parameters of Fig. 1. Illustrated is an isosurface where $|\mathbf{\Lambda}_+|^2$ equals 50% of its maximum value in the box. Higher energy levels are concentrated within two (opposite polarity) fat tubes.

produces an equilibrium with $\mathbf{U} = \epsilon\mathbf{U_0} + \mathbf{B_0}$ and $\mathbf{B} = \mathbf{B_0}$. We investigated this in a computation described in section 3.2, but first, we look at the case where we continue to use the forcing described by equation (1) with $\nu = \eta = 1/400$.

We started this calculation from $\mathbf{U} = \mathbf{B} = \mathbf{F}_\gamma/(2\nu)$, again with a small amount of added noise. The time evolution is more complicated, as is shown in Fig. 4. The spatial structure at $t = 6385$ and at $t = 7157$ is shown in Figs 5 and 6. Although in Cameron & Galloway (2005) we found that $\nu(\sin z, \sin x, \sin y)$ leads to the Archontis family of dynamos, the theory does not predict that a force scaling with ν should always produce a family of steady $\mathbf{U} \sim \mathbf{B}$ dynamos. So the fact that something different happens here is unremarkable. What is surprising is that the solution has $\mathbf{U} \sim \mathbf{B}$ over an extended period, even though both $\mathbf{U}$ and $\mathbf{B}$ vary significantly and apparently chaotically. We can understand such time-

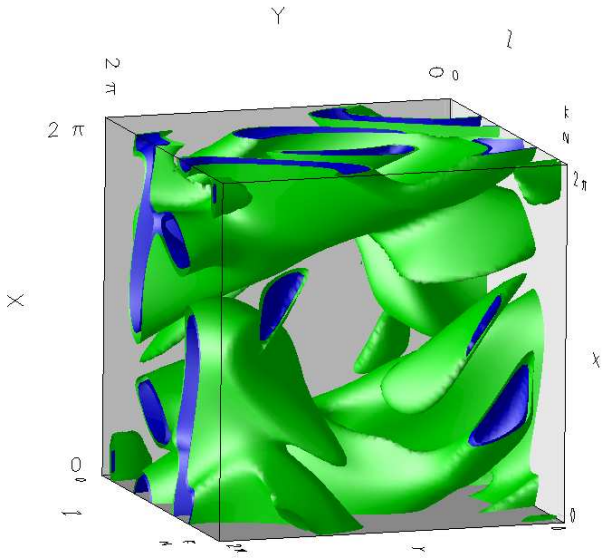

Figure 3. Similar to Fig 2, except that $\mathbf{\Lambda}_-$ is shown.

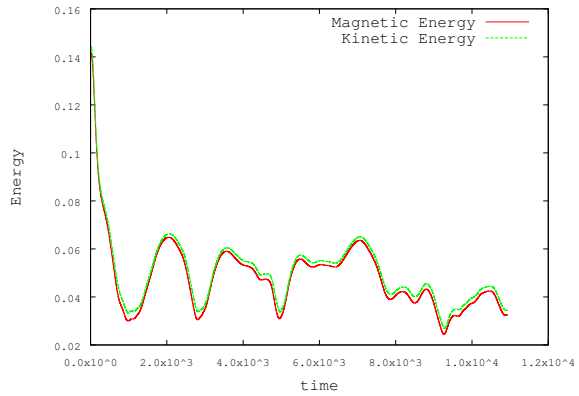

Figure 4. Time development of the magnetic and kinetic energies for the case $\gamma = 0.125$, $A : B : C = 0.5 : 1 : 1$, $\nu = \eta = 1/400$.

dependent behaviour as follows, starting with the evolution equations written in Elsässer variables using the simplifying assumption $\eta = \nu$:

$$\frac{\partial \mathbf{\Lambda}_+}{\partial t} = -(\mathbf{\Lambda}_- \cdot \nabla)\mathbf{\Lambda}_+ + \nu\nabla^2\mathbf{\Lambda}_+ - \nabla P + \mathbf{F} \tag{11}$$

$$\frac{\partial \mathbf{\Lambda}_-}{\partial t} = -(\mathbf{\Lambda}_+ \cdot \nabla)\mathbf{\Lambda}_- + \nu\nabla^2\mathbf{\Lambda}_- - \nabla P + \mathbf{F} \tag{12}$$

$$\nabla \cdot \mathbf{\Lambda}_+ = 0 \tag{13}$$

$$\nabla \cdot \mathbf{\Lambda}_- = 0\ . \tag{14}$$

Letting $(\mathbf{\Lambda}_{+\nu_0}(t),\ \mathbf{\Lambda}_{-\nu_0}(t))$ describe the evolution of the system when $\nu = \nu_0$, $(\mathbf{\Lambda}_{+\nu_0}(\epsilon t),\ \epsilon\mathbf{\Lambda}_{-\nu_0}(\epsilon t))$ is an $O(\epsilon)$ approximate solution when $\nu = \epsilon\nu_0$, as can readily be confirmed by substitution. This argument is only suggestive, as there is no proper basis for ignoring the second order terms. Nonetheless, for small ϵ, time-dependent $\mathbf{U} \sim \mathbf{B}$ behaviour is not as surprising as it at first seems.

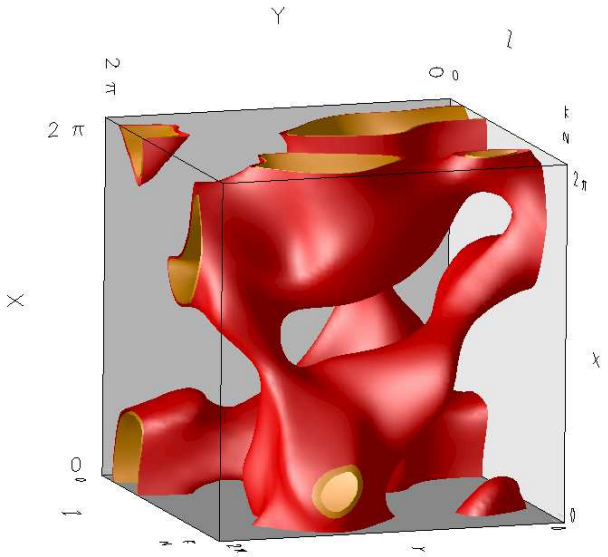

Figure 5. This figure shows $\mathbf{\Lambda}_+$ for the forcing $\mathbf{F}_\gamma = \nu\{A\sin z + C\gamma\cos y, B\sin x + A\gamma\cos z, C\sin y + B\gamma\cos x\}$, with $A:B:C = 0.5:1:1$, $\gamma = 0.125$ and $\nu = \eta = 1/400$ at $t = 6358$. The isosurface is at the level where $|\mathbf{\Lambda}_+|^2$ reaches half its maximum value.

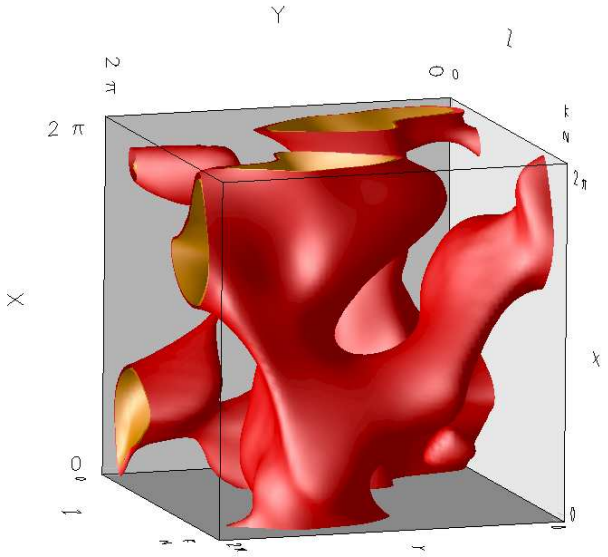

Figure 6. As for Fig 5 except the solution at $t = 7157$ is shown.

The numerical calculation was terminated at $t = 11000$ (27.5 diffusive timescales), since it is impossible to continue it indefinitely. We are thus unsure whether the solution would have eventually evolved to a steady state, remained chaotic, or even evolved away from a $\mathbf{U} \sim \mathbf{B}$ state into something completely different. For numerically derived solutions with a chaotic time-dependence this is always a problem - is the solution truly chaotic or merely in a long transient phase? (For an example where this issue is pursued in greater detail for the long-term stability of the (1,1,1) ABC flow, see Podvigina & Pouquet 1994.)

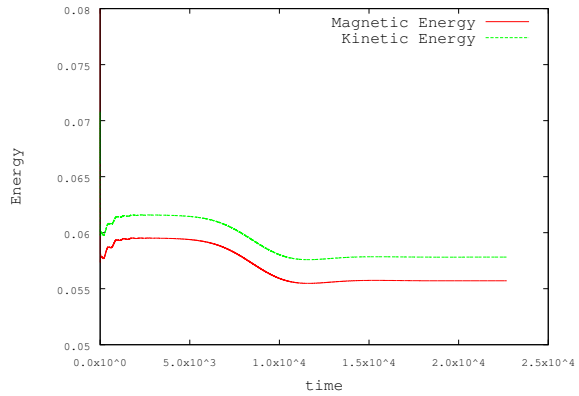

Figure 7. Time development of the magnetic and kinetic energies for the case where **F** is based on the equilibrium in Section 3.1 for $\nu = \eta = 1/100$, but the diffusivities have been changed to $\nu = \eta = 1/400$. The initial condition is perturbed as described in the text. By construction there is a new equilibrium which begins to appear for $0 < t < 5000$, but which is unstable and subsequently evolves to a different nearby stable steady state.

3.2 Results using a forcing based on the dynamo of Section 3.1

Cameron & Galloway (2005) described how to generate a series of stationary equilibria from any steady dynamo. In this section we use the solution obtained for $\nu = \eta = 1/100$ in section 3.1 to generate a steady state with $\nu = \eta = 1/400$. The newly generated equilibrium $\mathbf{\Lambda}_-$ is constructed to be exactly as shown in Fig 3, reduced in amplitude by a factor of 4. The magnetic field is identical to that when $\nu = \eta = 1/100$. Both the velocity field and $\mathbf{\Lambda}_+$ can then be determined from these two quantities. The interesting question is whether the new steady state is stable.

To answer this, we set up the new equilibrium numerically, and then subjected it to a perturbation. The resulting time evolution is shown in Fig 7. At first the magnetic energy approaches 0.06. This is the level corresponding to the constructed state (see Fig. 1). However, for $t > 5000$ the evolution is towards a new state with lower energy. The constructed equilibrium is unstable, but interestingly the system evolves to a nearby steady state which is stable. This behaviour was confirmed using several different perturbations.

The spatial structure of the stable equilibrium shown in Fig 8 differs only slightly from that shown in Fig 2. To understand the changes we consider the difference between $\mathbf{\Lambda}_-$ in the two equilibria, which is shown in Fig. 9. This figure shows the changes are concentrated into 'cigars' and sheets associated with stagnation points. Using a program which traces field lines, we have confirmed that these cigars are related to the streamlines of unstable 1-D manifolds associated with certain stagnation points. The latter do not connect in any simple way to nearby stagnation points, and so are not heteroclinic orbits of the type associated with the Archontis dynamo.

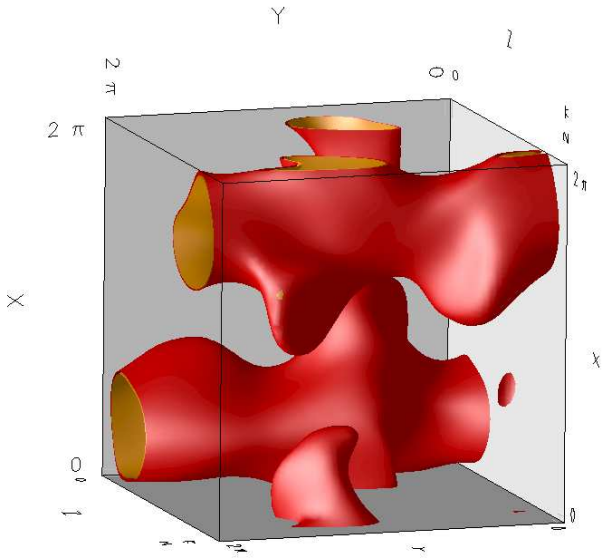

Figure 8. Equilibrium structure of $\mathbf{\Lambda}_+$ for the stable solution present at the end of the run shown in Figure 7.

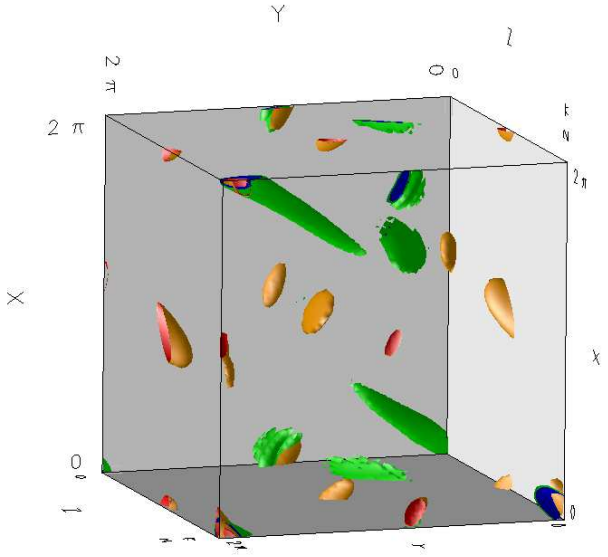

Figure 9. As for Fig 8 except that the difference between $\mathbf{\Lambda}_-$ between the initial and final equilibria is shown. The isosurface is at 70% of the maximum magnitude of the difference and appears blue/green. For comparison the red/orange surface shows where $|\ \mathbf{U}\ |$ is less than 1.2% of its maximum value – and hence shows the location of the stagnation points. The difference between the two solutions is seen to be primarily concentrated in a cigar associated with the stagnation point near (0,0,0). The periodicity means the latter also appears near $(0, 0, 2\pi)$, $(0, 2\pi, 0)$, $(0, 2\pi, 2\pi)$, and so on.

The fact that the constructed equilibrium is unstable in the neighbourhood of the 1-D unstable manifolds is readily understood from the analysis in Cameron & Galloway (2005), where the stability argument was constructed by ignoring $O(\nu^2)$ terms. This is justified everywhere except near these manifolds, which are structures where the $O(\nu)$ terms actually vanish. The existence of the second equilibrium shows that there are possible changes localised around these regions which do not affect the dynamo's large-scale structure and which allow a stable solution to emerge. We will explain this qualitatively in the next section.

4 A MODIFIED ROTOR DYNAMO

The first proof that fluid motions could sustain a magnetic field was provided by Herzenberg (1958). It was a constructive proof, providing an analytic example of a dynamo featuring two rotating spheres immersed in a fluid otherwise at rest. For simplicity we restrict our attention here to a similar but more transparent version where there are three rotating spheres (Gibson 1968b). The theory is discussed in detail in the books by Roberts (1967) and Moffatt (1978) to which we refer the reader. A recent description of the kinematic problem is due to Brandenburg et al. (1998), who also discuss a number of other configurations for the spheres and extend the treatment to include oscillatory solutions.

Here we are interested solely in steady solutions, and in this paragraph and the next we summarise the description in Moffatt (1978) of the problem solved by Gibson (1968b). The configuration consists of three conducting spheres of radius a embedded in a non-moving conducting medium. The spheres ($S_{1,2,3}$) are positioned at $\mathbf{x_1} = (d, 0, 0)$, $\mathbf{x_2} = (0, d, 0)$ and $\mathbf{x_3} = (0, 0, d)$. They each undergo rigid rotation, so that the velocity field is

$$\mathbf{U}(\mathbf{x}) = \left\{ \begin{array}{c} \boldsymbol{\omega_i} \times (\mathbf{x} - \mathbf{x_i}) \text{ for } |\mathbf{x} - \mathbf{x_i}| < a \\ 0 \text{ elsewhere} \end{array} \right\} \ , \tag{15}$$

where $\boldsymbol{\omega_1} = (0, 0, -\omega)$, $\boldsymbol{\omega_2} = (-\omega, 0, 0)$, and $\boldsymbol{\omega_3} = (0, -\omega, 0)$. The fluid outside the spheres has $\mathbf{U} = \mathbf{0}$. The problem is linear in the magnetic field, and when $a << d$ an analytic expression exists for the eigenmode with the highest growth rate.

The characteristic velocity and length-scale for this system are ωa and a respectively, so that the magnetic Reynolds number is $\mathrm{Rm} = \omega a^2/\eta$. Gibson (1968b) showed that this flow acts as a dynamo if $\mathrm{Rm} \geqslant 5(d\sqrt{2}/a)$. The special case $\mathrm{Rm} = 5(d\sqrt{2}/a)$ creates a stationary dynamo, where the magnetic field neither grows nor decays. We can now apply the scaling arguments of Cameron & Galloway (2005) using this as our example of a steady state solution to the induction equation.

We let $\mathbf{U_0}$ be the velocity defined above, for $\nu = \nu_0$, and $\mathbf{B_0}$ be the stationary magnetic field. The amplitude of $\mathbf{B_0}$ is arbitrary. We can now generate an equilibrium solution of equations (5)–(8) for $\nu = \epsilon\nu_0$ and $\eta = \epsilon\eta_0$. This solution is

$$\mathbf{U_1} = \epsilon\mathbf{U_0} + \mathbf{B_0} \tag{16}$$

$$\mathbf{B_1} = \mathbf{B_0} \ , \tag{17}$$

and the force that needs to be provided in the momentum equation to drive it is

$$\mathbf{F} = \epsilon^2(\mathbf{U_0} \cdot \nabla \mathbf{U_0} - \nu_0 \nabla^2 \mathbf{U_0}) + 2\epsilon \mathbf{B_0} \cdot \nabla \mathbf{U_0} \ . \tag{18}$$

This dynamo has the property that $\mathbf{U} \to \mathbf{B}$ as ν and $\eta \to 0$. For small ϵ the flow is completely dominated by $\mathbf{B_0}$, which now defines the characteristic velocity, and the characteristic length-scale becomes d, because that is the scale on which $\mathbf{B_0}$ varies. Thus the Reynolds number becomes $\frac{1}{\epsilon}\frac{|\mathbf{B_0}|d}{\nu_0}$ and the magnetic Reynolds number is $\frac{1}{\epsilon}\frac{|\mathbf{B_0}|d}{\eta_0}$. Since $\mathbf{B_0}$, d and ν_0 are fixed these both tend to infinity as ϵ tends to zero.

4.1 Structure near the spheres

Although the spheres are essential for the generation of the magnetic field, their exact internal structure is not critical. Moffatt (1978) demonstrates that the only quantity of importance for the field away from the sphere is

$$\bar{\omega} = 5 \int_0^a r^4 \omega(r) dr / a^5 \ . \tag{19}$$

Thus instead of the spheres being rigidly rotating, we could have arbitrarily chosen a rotation profile and adjusted its amplitude to satisfy equation (19). Furthermore we could have easily changed the radius of the sphere without affecting the large-scale field, again by adjusting the rotation rate.

This insensitivity to the structure within the spheres corresponds to the fact that varying η and ν produces only localised changes near the 1-D unstable manifolds, for both the numerical example studied in section 3.2 and the Archontis dynamo studied in Cameron & Galloway (2005). The large-scale structure of the magnetic field away from these regions remains unaltered. Given this decoupling, it is not surprising that the constructed solution of section 3.2 is unstable and evolves to a nearby solution. The changes reflect the fact that $\mathrm{Re}^{-1/2}$ and $\mathrm{Rm}^{-1/2}$ are the natural thicknesses of boundary layers. These solutions are free to modify themselves locally so that they can adopt the appropriate thickness near the stagnation points, 1-unstable manifolds, and heteroclinic orbits, without affecting what happens in the bulk of the fluid. This also explains the insensitivity of the large-scale field to the magnetic Prandtl number $Pm = \nu/\eta$ seen in the context of the Archontis dynamo.

Whilst the choice of spheres is mathematically convenient, physical experiments using rotating cylinders have been carried out by Lowes & Wilkinson (1968). These cylinders are probably a closer model for the boundary layers that form surrounding the 1-D heteroclinic

orbits (in the case of the Archontis dynamo), or the 1-D unstable manifolds (for the modified ABC dynamo).

5 CONCLUSION

We have presented a second numerical example of a stable dynamo which has $\mathbf{U} \to \mathbf{B}$ as Re and Rm $\to \infty$. The existence of families of such dynamos was demonstrated in Cameron & Galloway (2005), but as we have only heuristic arguments regarding their stability, additional examples are necessary in order to develop experience as to whether they are likely to be common or not. In this paper, we have only given details of one example, for one particular value of our parameter γ. Whilst we have yet to conduct a systematic study, preliminary experiments with nearby values gave similar results.

We have also made progress in understanding the behaviour near stagnation points and their 1-D unstable manifolds. In both the kinematic sines- and 1:1:1 ABC-flows, these features are closely related to fast dynamo action, and the structure of the flow near these regions is of great importance. $\mathbf{U} \sim \mathbf{B}$ dynamos are different; they are sensitive only to integrated effects from these regions, as is shown in equation (19). This difference explains why the magnetic field of the Archontis flow is time independent even though the flow differs only slightly from that of a fast dynamo (Cameron & Galloway 2005). It also helps us to understand the stability of these dynamos. The arguments given in our earlier paper apply only when terms of order ν^2 are ignorable, which is not the case near the stagnation points and 1-D manifolds. This paper has now shown that the flow structure in these regions does not have a major impact provided $\bar{\omega}$, defined in equation (19), is unchanged.

We have also discussed a new class of dynamos, which are time-dependent solutions with $\mathbf{U} \sim \mathbf{B}$. An example where $\nu = \eta = 1/400$ was described. The variations occur on the slow, diffusive timescale, and an argument has been given to suggest why such solutions might be expected. An outstanding problem for all $\mathbf{U} \sim \mathbf{B}$ dynamos found so far is that the evolution proceeds on this slow timescale. The kinematic fast dynamo problem has now become a dynamic one: are there dynamos which can reach a strong field state on the fast turnover timescale rather than the diffusive timescale? The presence of turbulence in most astrophysical objects also casts doubt on whether it is appropriate to take the enormously long laminar diffusion timescales literally when considering this problem.

The procedures outlined in this and our earlier paper enable a large number of numerical

and analytical stationary dynamos to be created. As far as existence is concerned, there is no restriction on how much total magnetic energy can be sustained relative to kinetic energy—it is simply a matter of providing the right driving force in the momentum equation. When the magnetic and kinetic energies are equal, a number of these dynamos appear stable in numerical experiments; an explanation of the stability which is valid away from the stagnation points and their stable or unstable manifolds has been given in Cameron & Galloway (2005). The behaviour near these structures, and the way they couple to the large-scale field, have both been dealt with here, thus giving a more complete picture of these strong-field dynamos. The ease with which they can be constructed, at least in the model cases studied here, gives some hope that such dynamos may actually exist in the Universe, and we encourage observers to see whether they can find them.

ACKNOWLEDGEMENTS

DJG thanks the Isacc Newton Institute for Mathematical Sciences, Cambridge, UK, for the opportunity to participate in the program "Magnetohydrodynamics of Stellar Interiors". Both authors would like to acknowledge helpful comments from Andrew Gilbert and Mike Proctor.

REFERENCES

Archontis V., 2000, PhD thesis, University of Copenhagen

Archontis V., Dorch S. B. F., Nordlund A., 2005, A&A, in preparation

Beck R., 2002, 275, 331

Blackman E., 2002, in Falgarone E., Passot T., eds, Turbulence and Magnetic Fields in Astrophysics Vol. 614 of Springer Lecture Notes in Physics. Springer, Berlin, pp 432–463

Blackman E. G., Field G. B., 2002, Physical Review Letters, 89, 265007

Brandenburg A., 1994, in Proctor M. R. E., Gilbert A., eds, Lectures on Solar and Planetary Dynamos Publications of the Newton Institute. Cambridge University Press, Cambridge, pp 117–159

Brandenburg A., 2001, ApJ, 550, 824

Brandenburg A., Moss D., Soward A. M., 1998, Royal Society of London Proceedings Series A, 454, 1283

Cameron R., Galloway D., 2005, MNRAS, accepted

Diamond P. H., Hughes D. W., Kim E.-J., 2005, in Soward A. M., Jones C. A., Hughes D. W., Weiss N. O., eds, Fluid dynamics and dynamos in astrophysics and geophysics Vol. 12 of The fluid mechanics of astrophysics and geophysics. CRC Press, Boca Raton, FL., pp 145–192

Dorch S. B. F., Archontis V., 2004, Sol. Phys., 224, 171

Galanti B., Sulem P. L., Pouquet A., 1992, Geophys. Astrophys. Fluid Dyn., 5158, 1

Gibson R. D., 1968a, Q. J. Mech. Appl. Math., 21, 243

Gibson R. D., 1968b, Q. J. Mech. Appl. Math., 21, 257

Glatzmaier G. A., Roberts P. H., 1995, Nat, 377, 203

Gruzinov I., Diamond P. H., 1994, Physical Review Letters, 72, 1651

Haugen N. E. L., Brandenburg A., Dobler W., 2004, Ap&SS, 292, 53

Herzenberg A., 1958, Phil. Trans. Roy. Soc. A, 249, 507

Hughes D. W., 1993, in Proctor M. R. E., Matthews P. C., Rucklidge A. M., eds, Solar and Planetary Dynamos Publications of the Newton Institute. Cambridge University Press, Cambridge, pp 153–159

Lowes F. J., Wilkinson I., 1968, Nat, 198, 1158

Maron J., Cowley S., McWilliams J., 2004, ApJ, 603, 569

Moffatt H. K., 1978, Magnetic field generation in electrically conducting fluids. Cambridge University Press, Cambridge

Podvigina O., Pouquet A., 1994, Physica D, 75, 471

Roberts P. H., 1967, An introduction to Magnetohydrodynamics. American Elsevier, New York

Steiner O., Ferriz-Mas A., 2005, Astronomische Nachrichten, 326, 190

Vainshtein S. I., Cattaneo F., 1992, ApJ, 393, 199